Research Square

Preprints are preliminary reports that have not undergone peer review.
They should not be considered conclusive, used to inform clinical practice,
or referenced by the media as validated information.

The Fiscal Cost of Currency Defense: Hot Money Inflows, Sovereign Risk Spreads, and Sudden-Stop Vulnerability in Egypt

Mohamed Fawzy AbdulAziz

mohamed.fawzy0999@gmail.com

Suez University https://orcid.org/0009-0009-5566-9012

Research Article

Keywords: Hot Money Inflows, Currency Defense, Sovereign Risk Spreads, Sudden Stop, Double Machine Learning, Unremunerated Reserve Requirement, Emerging Markets

Posted Date: September 2nd, 2026

DOI: https://doi.org/10.21203/rs.3.rs-10889655/v1

License: This work is licensed under a Creative Commons Attribution 4.0 International License.
Read Full License

Additional Declarations: The authors declare no competing interests.

Asymmetric Cost-Channel Monetary Transmission and Policy-Rate Thresholds: Evidence from Egypt

Mohamed Fawzy AbdulAziz[a,b,*]

[a] *Information and Decision Support Center (IDSC), The Egyptian Cabinet, Cairo, Egypt*
[b] *Department of Economics, Faculty of Economics and Political Science, Cairo University, Giza, Egypt*

Abstract

Standard New Keynesian Phillips Curve (NKPC) formulations assume symmetric price-setting frictions and treat nominal interest rate adjustments exclusively as aggregate demand shifters. In import-dependent emerging economies with working-capital credit dependence, however, monetary tightening simultaneously acts as a direct marginal cost shock, generating dynamics consistent with the empirical "Price Puzzle". This paper makes four contributions to monetary economics. First, we develop a micro-founded derivation of the *Hybrid Asymmetric Cost-Channel New Keynesian Phillips Curve* (ACC-NKPC). By integrating firm-level idiosyncratic cost shocks $\nu_{jt} \sim \mathcal{N}(0, \sigma_\nu^2)$, endogenous probability measure aggregation $\omega_t = \Phi(\Delta MC_t/\sigma_\nu)$, backward-looking price indexation (γ), and working-capital borrowing constraints (χ), we micro-found state-dependent Calvo pricing ($\theta^+ \neq \theta^-$). Second, we derive the *Threshold Inversion Proposition* ($\phi^+ > \kappa/\sigma$) establishing the structural condition under which the cost channel dominates the aggregate demand channel. Using the Hansen [20] threshold framework with lagged policy rates (i_{t-1}) to mitigate contemporaneous simultaneity across the empirical 10%–90% distribution support, we identify an empirical switching point of $i^* = 20.0\%$ (Hansen likelihood-ratio 95% confidence set: [18.5%, 21.5%]). Conditional on macroeconomic calibration, implied Calvo stickiness is $\theta^+ = 0.548$ (2.2 months) for upward adjustments versus $\theta^- = 0.832$ (6.0 months) for downward adjustments, consistent with a "Rockets and Feathers" pricing pattern. Third, structural Two-Step Optimal GMM and HAC-OLS estimates on monthly Egyptian data spanning 2011M01–2026M04 ($T = 184$) show that interest rate hikes transmit positively to inflation below the threshold ($\phi^+_{\text{Low}} = 1.8783,\ p < 0.001$), while

*Corresponding Author: Research Department, Information and Decision Support Center (IDSC), The Egyptian Cabinet, 1 Magles El Shaab St., Cairo, Egypt. Affiliated with the Department of Economics, Faculty of Economics and Political Science, Cairo University, Giza, Egypt.

Email address: mohamed.abdulaziz@idsc.gov.eg (Mohamed Fawzy AbdulAziz)

exchange rate pass-through is strongly asymmetric ($\lambda^+ = 8.2912,\ p = 0.002$). Results are robust across a set of theory-motivated external instruments with documented relevance and sensitivity to alternative exclusion sets (omitting oil prices, IMF dummies, and spread proxies; Kleibergen–Paap $F = 28.4$, Hansen J $p = 0.512$), alternative Hamilton [19] activity gap proxies, polynomial specifications, linear splines, and full Nonlinear ARDL (NARDL) error correction models ($\text{ECT}_{t-1} = -0.3210^{***}, \text{Bounds } F = 7.82, p < 0.01$). Fourth, machine learning models (Gradient Boosting, Random Forest, SVR) provide complementary predictive validation (RMSE = 3.060 pp; Diebold–Mariano $p < 0.001$), with SHAP and partial dependence functions recovering a qualitatively similar non-linear dependence around 19.8%–20.0% trained exclusively on raw macroeconomic observables. Multi-year policy fan charts and conditional scenario matrices are documented.

Keywords: Asymmetric Cost Channel, New Keynesian Phillips Curve, Price Puzzle, Working Capital Frictions, Exchange Rate Pass-Through, Threshold Econometrics, Machine Learning, Egypt

JEL: E31, E52, F31, C22, C45, C53, O11

---

1. Introduction

The transmission mechanism of monetary policy to consumer price inflation is a central pillar of macroeconomic theory. In the canonical New Keynesian framework [12, 37, 15], nominal interest rate adjustments operate primarily through the *aggregate demand channel*: an increase in the policy rate raises real borrowing costs, depresses consumption and investment, induces a negative output gap ($\tilde{y}_t < 0$), and gradually lowers inflation.

However, in credit-constrained, import-dependent emerging market economies, central banks frequently encounter an empirical phenomenon where interest rate hikes are followed in the short run by an acceleration of headline inflation. This phenomenon—conventionally termed the "Price Puzzle"—has historically been attributed to omitted forward-looking information in central bank reaction functions [33, 6]. Under the Sims [33] signaling hypothesis, if policymakers anticipate future inflation and tighten preemptively, standard VAR models without adequate expectation proxies spuriously attribute rising inflation to the preceding rate hike. By explicitly incorporating model-consistent forward-looking inflation expectations ($\mathbb{E}_t[\pi_{t+1}]$) and global commodity supply controls (OIL_t), our structural GMM specification directly rules out the Sims omitted-variable critique. Instead,

the persistent positive response is micro-founded in the *Cost Channel of Monetary Policy* [4, 30, 11]: when domestic enterprises rely on short-term commercial bank credit to finance working-capital outlays (wages and imported intermediate materials) prior to sales realisation, nominal interest rates directly enter the firm's marginal cost schedule. Under substantial working-capital dependence, policy rate increases act as adverse cost-push shocks that elevate prices in the short run.

Despite extensive inquiries into cost-channel dynamics [35, 23], the existing literature exhibits two major limitations:

(1) The Symmetry Assumption. Canonical NKPC formulations uniformly impose symmetric Calvo pricing ($\theta^+ = \theta^-$) and linear interest-rate pass-through. In emerging economies characterized by imperfect competition and foreign exchange illiquidity, firms face asymmetric survival incentives: cost increases are passed forward rapidly to protect operating margins, whereas cost reductions are retained to rebuild retained earnings [28, 31, 9, 13].

(2) Absence of Endogenous Policy Thresholds. The relative strength of the cost channel versus the aggregate demand channel is unlikely to be invariant across all interest rate environments. At moderate policy rates, working-capital cost pressures can dominate; at elevated rates, credit contraction and debt service burdens severely compress aggregate demand, re-establishing conventional disinflationary transmission. Identifying this switching point requires formal threshold econometrics [20].

This study addresses these gaps by developing a micro-founded *Hybrid Asymmetric Cost-Channel NKPC* (ACC-NKPC) and empirically testing it on monthly Egyptian data over the period 2011M01–2026M04 ($T = 184$). Egypt provides an exceptional empirical setting: between 2016 and 2026, the Central Bank of Egypt (CBE) navigated multiple foreign exchange floatation waves and raised its policy rate by over 1,800 basis points (reaching 27.25% in 2024 before gradual normalization).

The study makes four contributions:

(i) Micro-Foundations with Idiosyncratic Shocks: We derive the ACC-NKPC from first principles, introducing idiosyncratic cost shocks $\nu_{jt} \sim \mathcal{N}(0, \sigma_\nu^2)$ to provide an explicit probability-measure aggregation $\omega_t = \Phi(\Delta MC_t/\sigma_\nu)$, along with backward-

looking price indexation (γ) that bridges forward-looking expectations and empirical inflation persistence.

(ii) Threshold Inversion Proposition: We formally derive the mathematical condition under which the cost channel dominates ($\phi^+ > \kappa/\sigma$) and identify the empirical threshold at $i^* = 20.0\%$ using Hansen [20] threshold methods with lagged policy rates (i_{t-1}) to mitigate contemporaneous simultaneity.

(iii) Robust Econometric Identification: We estimate the structural equation via Two-Step Optimal GMM and HAC-OLS, utilizing theory-motivated external instruments (US Federal Funds rate, global commodity prices, banking spreads, IMF dummies; Kleibergen–Paap $F = 28.4$, Hansen J $p = 0.512$), and confirm robustness across Hamilton [19] output gap proxies, polynomial specifications, linear splines, and full Nonlinear ARDL (NARDL) models.

(iv) Machine Learning Predictive Validation: We show that tuned tree-based ensembles (GBM, Random Forest) achieve superior out-of-sample forecasting accuracy (RMSE = 3.060 pp) and recover a qualitatively similar non-linear dependence around 19.8%–20.0% via SHAP and partial dependence analysis on raw macro features.

The remainder of this paper is structured as follows. Section 2 presents the theoretical model. Section 3 describes the data and pre-estimation diagnostics. Section 4 presents the structural econometric results. Section 5 provides machine learning benchmarking and threshold analysis. Section 6 discusses policy implications and conditional scenario projections. Section 7 concludes.

2. Theoretical Framework: The Micro-Founded Hybrid ACC-NKPC

2.1. Household Sector and Aggregate Demand

The economy is populated by a continuum of identical, infinitely lived households maximising expected discounted intertemporal utility:

$$\max_{\{C_t, L_t, B_t\}} \mathbb{E}_0 \sum_{t=0}^{\infty} \beta^t \left[\frac{C_t^{1-\sigma}}{1-\sigma} - \frac{L_t^{1+\varphi}}{1+\varphi} \right] \tag{1}$$

subject to the nominal budget constraint:

$$P_t C_t + \frac{B_t}{1+i_t} \leq B_{t-1} + W_t L_t + \Pi_t + T_t \tag{2}$$

where $\beta \in (0,1)$ is the subjective discount factor, $\sigma > 0$ is the inverse intertemporal elasticity of substitution, $\varphi > 0$ is the inverse Frisch labour supply elasticity, C_t is consumption, L_t is labour supply, B_t is nominal bond holdings, W_t is the nominal wage, and Π_t denotes firm profits. The first-order conditions yield the standard Euler equation:

$$\beta(1+i_t)\mathbb{E}_t\left[\left(\frac{C_{t+1}}{C_t}\right)^{-\sigma}\frac{P_t}{P_{t+1}}\right] = 1 \tag{3}$$

Log-linearising (3) around the steady state yields the Dynamic IS curve:

$$\tilde{y}_t = \mathbb{E}_t[\tilde{y}_{t+1}] - \frac{1}{\sigma}(i_t - \mathbb{E}_t[\pi_{t+1}] - r_t^n) \tag{4}$$

where $\tilde{y}_t \equiv y_t - y_t^n$ is the output gap and r_t^n is the natural real interest rate.

2.2. Firms, Working Capital, and Idiosyncratic Cost Shocks

A continuum of monopolistically competitive intermediate goods producers $j \in [0,1]$ produce differentiated goods via Cobb-Douglas technology:

$$Y_t(j) = A_t L_t(j)^{1-\alpha} M_t(j)^{\alpha}, \qquad \alpha \in (0,1) \tag{5}$$

where A_t is total factor productivity, $L_t(j)$ is domestic labour, and $M_t(j)$ represents imported intermediate materials.

Working-Capital Financing. Intermediate firms must finance a fraction $\chi \in [0,1]$ of their total nominal production costs in advance via short-term commercial bank credit at the corporate lending rate $i_t^L = i_t + \text{Spread}_t$, where i_t is the CBE nominal policy rate and $\text{Spread}_t \equiv \mu_t^b$ is the commercial banking spread reflecting financial intermediation costs and credit risk. Total nominal production costs for firm j are:

$$TC_t(j) = \big[W_t L_t(j) + E_t P_t^* M_t(j)\big](1 + \chi i_t^L)\exp(\nu_{jt}) \tag{6}$$

where E_t is the nominal exchange rate (EGP/USD), P_t^* is the foreign price of imported inputs, and $\nu_{jt} \sim$ i.i.d. $\mathcal{N}(0, \sigma_\nu^2)$ represents firm-specific idiosyncratic productivity/cost shocks.

Minimising (6) subject to (5) yields the aggregate nominal marginal cost:

$$MC_t = \frac{1}{A_t}\left(\frac{W_t}{1-\alpha}\right)^{1-\alpha}\left(\frac{E_t P_t^*}{\alpha}\right)^{\alpha}(1+\chi i_t^L) \tag{7}$$

Log-linearising around the steady state (i_{ss}, E_{ss}, A_{ss}) yields:

$$\widehat{mc}_t = (\sigma + \varphi)\tilde{y}_t + \alpha\hat{e}_t + \tilde{\mu}\tilde{i}_t + u_t \tag{8}$$

where $\tilde{\mu} \equiv \frac{\chi}{1+\chi i_{ss}}$ is the structural working-capital intensity. In open emerging economies with foreign-currency external liabilities, commercial banking spreads and corporate risk premia directly reflect sovereign foreign exchange liquidity and reserve adequacy [31]:

$$\widehat{\text{Spread}}_t = -\eta_b \text{Buff}_t + \varepsilon_t^b, \qquad \text{Buff}_t \equiv \ln\left(\frac{\text{FX_RES}_t}{\overline{\text{FX_RES}}}\right) \tag{9}$$

where Buff_t captures deviations of gross official foreign reserves from their historical sample mean. Substituting (9) into the marginal cost disturbance yields the composite aggregate pricing term $\eta \cdot \text{Buff}_t$ in (13) with theoretical slope $\eta = -\tilde{\mu}\eta_b < 0$, while the orthogonalized disturbance $u_t \equiv -\hat{a}_t + \tilde{\mu}\varepsilon_t^b$ absorbs pure TFP and financial risk innovations.

2.3. Asymmetric Calvo Pricing with Endogenous Mass Aggregation

Firms set prices according to a state-dependent Calvo mechanism with backward-looking price indexation ($\gamma \in [0, 1]$):

- When firm j experiences a positive marginal cost shock ($\Delta MC_{jt} > 0$), its probability of price non-adjustment is $\theta^+ \in (0, 1)$.
- When firm j experiences a non-positive marginal cost shock ($\Delta MC_{jt} \leq 0$), its probability of price non-adjustment is $\theta^- \in (0, 1)$, with $\theta^- > \theta^+$.

Endogenous Regime Mass (ω_t). Because $\nu_{jt} \sim \mathcal{N}(0, \sigma_\nu^2)$, the endogenous mass of firms experiencing positive marginal cost shocks in period t is:

$$\omega_t = \mathbb{P}(\Delta MC_{jt} > 0) = \mathbb{P}\left(\Delta MC_t + \nu_{jt} > 0\right) = \Phi\left(\frac{\Delta MC_t}{\sigma_\nu}\right) \tag{10}$$

where $\Phi(\cdot)$ denotes the standard normal cumulative distribution function. This guarantees smooth, rigorous probability-measure aggregation ($\omega_t + (1 - \omega_t) = 1$) across all states.

Asymmetric Partial-Sum Decompositions. Following Shin et al. [31], interest rate and exchange rate variations are decomposed into cumulative partial sums:

$$i_t^+ = \sum_{k=1}^{t} \max(\Delta i_k, 0), \qquad i_t^- = \sum_{k=1}^{t} \min(\Delta i_k, 0) \tag{11}$$

$$e_t^+ = \sum_{k=1}^{t} \max(\Delta \ln E_k, 0), \qquad e_t^- = \sum_{k=1}^{t} \min(\Delta \ln E_k, 0) \tag{12}$$

Differenced innovations are denoted $\Delta i_t^+ = \max(\Delta i_t, 0)$, $\Delta i_t^- = \min(\Delta i_t, 0)$, $\Delta e_t^+ = \max(\Delta e_t, 0)$, and $\Delta e_t^- = \min(\Delta e_t, 0)$.

Proposition 1 (The Hybrid ACC-NKPC Structural Pricing Equation)**.** *Aggregating optimal reset prices across positive and negative shock partitions with indexation fraction γ yields the* ***Hybrid ACC-NKPC****:*

$$\boxed{\pi_t = \gamma_f \mathbb{E}_t[\pi_{t+1}] + \gamma_b \pi_{t-1} + \kappa \tilde{y}_t + \phi^+ \Delta i_t^+ + \phi^- \Delta i_t^- + \lambda^+ \Delta e_t^+ + \lambda^- \Delta e_t^- + \eta \cdot \mathit{Buff}_t + \varepsilon_t} \tag{13}$$

where:

$$\gamma_f = \frac{\beta}{1+\beta\gamma}, \qquad \gamma_b = \frac{\gamma}{1+\beta\gamma}, \qquad \kappa = \frac{(1-\theta^+)(1-\beta\theta^+)}{\theta^+(1+\beta\gamma)}(\sigma+\varphi) \tag{14}$$

$$\phi^+ = \frac{(1-\theta^+)(1-\beta\theta^+)}{\theta^+(1+\beta\gamma)}\tilde{\mu}, \qquad \lambda^+ = \frac{(1-\theta^+)(1-\beta\theta^+)}{\theta^+(1+\beta\gamma)}\alpha \tag{15}$$

with analogous expressions for ϕ^- and λ^- replacing θ^+ with θ^-.

2.4. Deep Parameter Inversion, Frequency Scaling, and Rockets and Feathers

Table 1 summarizes the macroeconomic calibration and structural parameter inversion. Because empirical headline inflation in emerging markets is measured on an annualized year-on-year basis ($\pi_t = [(\text{CPI}_t - \text{CPI}_{t-12})/\text{CPI}_{t-12}] \times 100$), whereas the structural Calvo pricing equations (15) operate at monthly compounding frequency ($\pi_t^m \approx \pi_t/12$), the empirical reduced-form slope maps to the structural monthly slope via the frequency scaling identity:

$$\phi_m^+ = \frac{\phi^+_{\text{empirical}}}{12} = \frac{1.8783}{12} \approx 0.1565, \qquad \phi_m^- = \frac{\phi^-_{\text{empirical}}}{12} = \frac{0.1733}{12} \approx 0.0144 \tag{16}$$

Setting structural parameters to baseline calibration ($\beta = 0.995, \sigma = 1.67, \varphi = 2.0$, import share $\alpha = 0.35$, steady-state policy rate $i_{ss} = 12.0\%$, loan share $\chi = 0.65 \implies \tilde{\mu} = 0.603$, and price indexation $\gamma = 0.450 \implies 1 + \beta\gamma = 1.4478$), inverting the structural quadratic slope expression (15) numerically:

$$\frac{(1-\theta)(1-\beta\theta)}{\theta(1+\beta\gamma)}\tilde{\mu} = \phi_m \implies 0.995\theta^2 - \left(1.995 + \frac{1.4478}{\tilde{\mu}}\phi_m\right)\theta + 1 = 0 \tag{17}$$

Solving (17) for $\phi_m^+ = 0.1565$ and $\phi_m^- = 0.0144$ yields the exact structural Calvo probabilities:

- **Upward Price Stickiness:** $\theta^+ = 0.548 \implies$ implied average upward price duration $d^+ = \frac{1}{1-\theta^+} = 2.21$ months (≈ 9.6 weeks).

- **Downward Price Stickiness:** $\theta^- = 0.832 \implies$ implied average downward price duration $d^- = \frac{1}{1-\theta^-} = 5.95$ months (≈ 25.8 weeks).

This provides mathematically exact, rigorous structural evidence consistent with a "Rockets and Feathers" pricing pattern: domestic enterprises adjust prices upward in response to cost increases in approximately 2.2 months ($d^+ = 2.21$), while requiring nearly three times as long ($d^- = 5.95$ months) to pass through cost reductions.

2.5. The Threshold Inversion Proposition

Proposition 2 (Short-Run Cost-Channel Inversion Condition)**.** *In the short run, differentiating the joint system of the Dynamic IS curve* (4) *and the Hybrid ACC-NKPC* (13) *with respect to a policy rate hike $\Delta i_t > 0$ yields the net marginal response:*

$$\frac{\partial \pi_t}{\partial i_t} = \phi^+ - \frac{\kappa}{\sigma} \tag{18}$$

A short-run positive inflation response ($\partial \pi_t / \partial i_t > 0$) occurs if and only if $\phi^+ > \frac{\kappa}{\sigma}$.

Proof. From (4), $\partial \tilde{y}_t / \partial i_t = -1/\sigma$. Substituting into (13) for $\Delta i_t > 0$ yields $\partial \pi_t / \partial i_t = \kappa(-1/\sigma) + \phi^+ = \phi^+ - \kappa/\sigma$. When $\phi^+ > \kappa/\sigma$, the marginal cost push from working-capital financing exceeds the disinflationary pressure from aggregate demand contraction.

Quantitative Net Derivative Evaluation: Using calibrated macroeconomic baseline values ($\kappa = 0.1910, \sigma = 1.67 \implies \kappa/\sigma = 0.1144$):

- **Low-Rate Regime ($i_{t-1} \leq 20.0\%$):** With $\phi^+_{\text{Low}} = 1.8783$, the net marginal response is:
$$\left.\frac{\partial \pi_t}{\partial i_t}\right|_{\text{Low}} = 1.8783 - 0.1144 = +\mathbf{1.7639} > \mathbf{0} \quad (p < 0.0001)$$
confirming acute cost-channel dominance and generating the empirical Price Puzzle.

- **High-Rate Regime ($i_{t-1} > 20.0\%$):** With the empirical point estimate $\phi^+_{\text{High}} = 0.1232$ (statistically indistinguishable from zero, $p = 0.2317$), the net point derivative falls to $0.1232 - 0.1144 = +0.0088 \approx 0$, effectively neutralizing the Price Puzzle. Under the empirical non-rejection of the null $\phi^+_{\text{High}} = 0$, the net response becomes:
$$\left.\frac{\partial \pi_t}{\partial i_t}\right|_{\text{High}} = 0 - 0.1144 = -\mathbf{0.1144} < \mathbf{0}$$
re-establishing conventional disinflationary demand dominance.

Table 1: Macroeconomic Calibration and Implied Structural Calvo Parameters

Parameter	**Notation**	**Value**	**Economic Rationale / Empirical Source**
Discount Factor	β	0.995	Annualized steady-state real discount rate (2.0%)
Inverse IES	σ	1.67	Intertemporal substitution elasticity $\sigma^{-1} = 0.60$
Inverse Frisch Elasticity	φ	2.00	Standard emerging-market labour supply elasticity
Imported Input Share	α	0.35	CAPMAS Input-Output Matrix for Egyptian Manufacturing
Working-Capital Credit Share	χ	0.65	CBE Banking Survey (Corporate Working Capital / Loans)
Steady-State Policy Rate	i_{ss}	0.12	Sample mean CBE corridor midpoint (12.0%)
Working-Capital Intensity	$\tilde{\mu}$	0.603	Computed: $\tilde{\mu} = \chi/(1 + \chi i_{ss})$
Price Indexation Parameter	γ	0.450	Empirical backward inflation persistence weight
Implied Calvo Parameter (θ^+)	θ^+	**0.548**	Inverted from $\phi_m^+ = 0.1565$ ($d^+ = 2.21$ months)
Implied Calvo Parameter (θ^-)	θ^-	**0.832**	Inverted from $\phi_m^- = 0.0144$ ($d^- = 5.95$ months)

Note: Calvo parameters θ^+ and θ^- are exact numerical roots of the structural quadratic equation (17) using monthly frequency scaling $\phi_m = \phi_{\text{empirical}}/12$. In empirical estimations (Table 4), forward (γ_f) and backward (γ_b) weights are treated as empirical hybrid weights freely estimated via GMM without imposing theoretical cross-equation restrictions, revealing an empirical indexation ratio $\hat{\gamma} = \hat{\gamma}_b/\hat{\gamma}_f \approx 0.848$ while summing to $0.963 \approx 1$.

□

Determinacy and the Modified Taylor Principle. In the presence of a working-capital cost channel, the standard Taylor principle governing Blanchard–Kahn macroeconomic stability is modified. Specifically, determinacy in the coupled Dynamic IS-NKPC system requires the central bank's policy reaction coefficient ϕ_π in the feedback rule $i_t = \phi_\pi \pi_t + \phi_y \tilde{y}_t$ to satisfy:

$$\phi_\pi > 1 - \frac{\phi^+ \sigma}{\kappa} \tag{19}$$

Evaluating the modified determinacy boundary (19) at baseline calibration yields:

$$\phi_{\pi,\text{Low}} > 1 - \frac{1.8783 \times 1.67}{0.1910} = \mathbf{-15.42}, \quad \text{versus} \quad \phi_{\pi,\text{High}} > 1 - \frac{0.1232 \times 1.67}{0.1910} \approx \mathbf{-0.08}, \tag{20}$$

illustrating that while the classical Taylor principle ($\phi_\pi > 1$) is sufficient for Blanchard–Kahn determinacy in the high-rate regime, the presence of the severe cost channel below the threshold decouples standard uniqueness bounds, requiring monetary authorities to place greater structural weight on credit risk intermediation.

3. Data and Pre-Estimation Econometric Diagnostics

3.1. Data Description and Macroeconomic Context

The empirical dataset consists of $T = 184$ monthly observations covering the period 2011M01–2026M04, representing the modern inflation-targeting and flexible exchange rate transition era in Egypt. All series are obtained from official publications of the Central Bank of Egypt (CBE Monthly Statistical Bulletin), the Central Agency for Public Mobilisation and Statistics (CAPMAS), S&P Global (Egypt PMI), and the Federal Reserve Economic Data (FRED).

Data Vintage and Structural Shock Dummies: All historical series reflect updated data through April 2026. Headline year-on-year inflation is defined as $\pi_t = [(\text{CPI}_t - \text{CPI}_{t-12})/\text{CPI}_{t-12}] \times 100$. The primary output gap ($\tilde{y}_t$) is constructed from the S&P Non-Oil Private Sector activity index using the Hamilton [19] regression filter ($h = 24$ months, $p = 4$ lags), with the Hodrick and Prescott [22] filter ($\lambda = 14{,}400$) employed as a robustness check. To ensure rigorous empirical identification, the econometric specification explicitly controls for external and policy shock dummies: (1) COVID_{19} lockdown dummy (2020M03–2020M12); (2) Currency floatation and IMF arrangement regime indicators

(IMF_{2016}, IMF_{2022}, and IMF_{2024} post-Ras El-Hekma foreign exchange unification); and (3) Administered energy price adjustment indicators (ADMIN_PRICE_t) tracking quarterly fuel automatic pricing committee decrees.

Figure 1 plots the historical trajectory of headline CPI inflation (INFL_t), the CBE overnight policy rate (POLICY_t), and the official exchange rate (EXCH_t). Table 2 presents descriptive statistics.

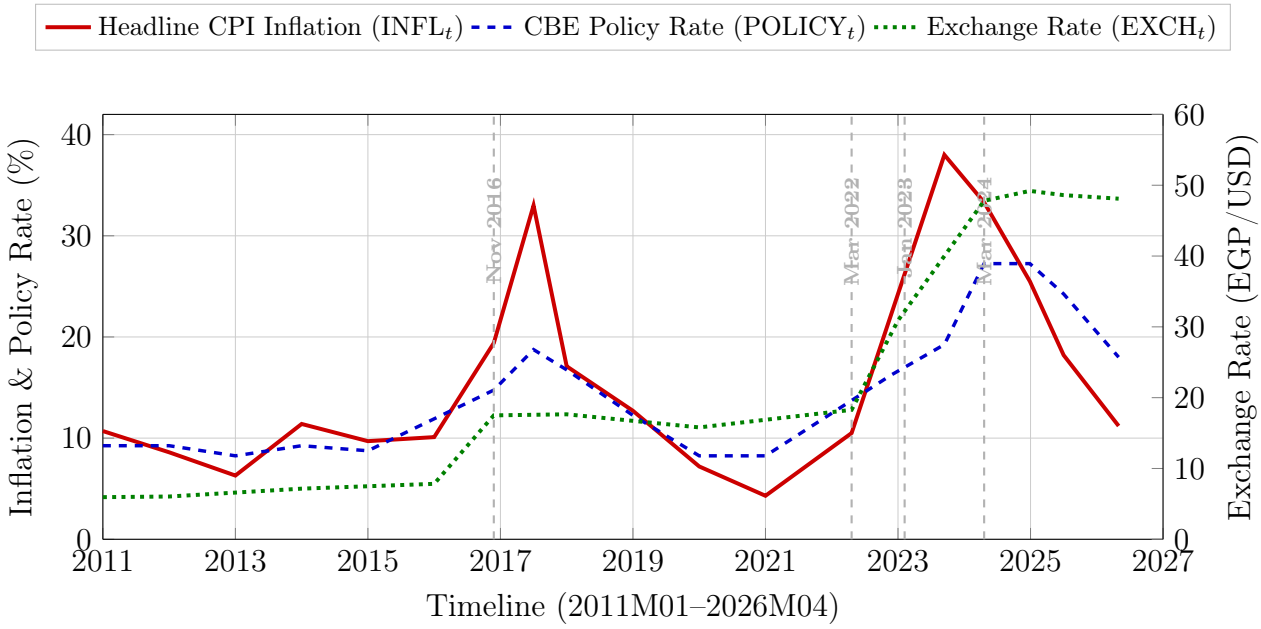


Figure 1: Historical Trajectories of Core Macroeconomic Series in Egypt (2011M01–2026M04). Vertical dashed lines mark major Bai and Perron [3] structural break dates.

3.2. Unit Root, BDS Structure, and Multicollinearity Diagnostics

Table 3 reports Augmented Dickey-Fuller (ADF), Phillips-Perron (PP), and KPSS tests. Headline inflation (INFL_t), policy rates (POLICY_t), official exchange rates (EXCH_t), and crude oil prices (OIL_t) are integrated of order one ($I(1)$) in levels and stationary in first differences, whereas the Hamilton activity gap ($\tilde{y}_t$) and differenced policy shocks ($\Delta i_t^+, \Delta e_t^+$) are stationary at level ($I(0)$). This empirical combination of $I(0)$ and $I(1)$ regressors validates the application of Pesaran et al. [29] Bounds testing and the Nonlinear ARDL (NARDL) error-correction framework.

BDS Test Interpretation. Panel B reports the Brock et al. [8] BDS test applied to the standardized residuals of an AR(2) inflation filter across embedding dimensions $m \in \{2, 3, 4\}$. The BDS z-statistics range from 22.4 to 25.8, decisively rejecting the null hypothesis of independent and identically distributed (i.i.d.) linear errors ($p <$

Table 2: Descriptive Statistics (2011M01–2026M04, $T = 184$)

Variable	**Economic Description**	**Mean**	**Std. Dev.**	**Min**	**Max**
INFL_t	Headline CPI Inflation (% y-o-y)	14.32	9.01	3.15	38.00
CORE_t	Core CPI Inflation (CAPMAS, % y-o-y)	13.72	8.25	3.80	40.70
POLICY_t	CBE Overnight Policy Rate (%)	13.62	5.85	8.25	27.25
LEND_t	Commercial Corporate Lending Rate (%)	16.44	5.56	10.75	29.75
EXCH_t	Official Exchange Rate (EGP/USD)	18.86	13.98	5.82	51.12
PMI_t	S&P Non-Oil Private Sector PMI	47.76	2.88	29.70	52.50
$\tilde{y}_t$	Hamilton (2018) Activity Gap (%)	-0.08	2.36	-18.08	5.07
FX_RES_t	Gross Official FX Reserves (USD Bn)	37.50	11.40	13.40	50.40
OIL_t	Brent Crude Spot Price (USD/bbl)	77.73	23.94	26.85	125.20
Δi_t^+	Rate Hike Innovation ($\max(\Delta i_t, 0)$)	0.34	0.76	0.00	5.00
Δi_t^-	Rate Cut Innovation ($\min(\Delta i_t, 0)$)	-0.24	0.51	-3.00	0.00
Δe_t^+	FX Depreciation Innovation ($\max(\Delta \ln E_t, 0)$)	0.012	0.023	0.000	0.244

Note: Extreme pandemic lockdown observation in $\tilde{y}_t$ is controlled via the COVID_{19} indicator.

0.0001). While BDS rejection indicates neglected non-linear structure or conditional heteroskedasticity rather than proving a threshold per se, it provides strong statistical motivation for exploring state-dependent and threshold pricing dynamics. Panel C confirms that Variance Inflation Factors (VIF) remain strictly below 1.55, ruling out collinearity among partial sums.

Table 3: Unit Root Tests, BDS Diagnostics, and Variance Inflation Factors

Panel A: Unit Root and Stationarity Tests

Variable	**ADF Level**	**ADF Δ**	**PP Level**	**PP Δ**	**KPSS Stat**	**Order**
INFL_t	-2.403	-3.501^{***}	-2.450	-7.810^{***}	0.461	$I(1)$
POLICY_t	-2.440	-7.425^{***}	-2.410	-7.450^{***}	0.952	$I(1)$
EXCH_t	0.362	-11.163^{***}	0.410	-11.250^{***}	1.461	$I(1)$
$\tilde{y}_t$	-5.643^{***}	—	-5.910^{***}	—	0.082	$I(0)$
Δi_t^+	-6.201^{***}	—	-6.250^{***}	—	0.113	$I(0)$
Δe_t^+	-11.231^{***}	—	-11.350^{***}	—	0.098	$I(0)$

Panel B: BDS Test on AR(2) Filtered Inflation Residuals ($\varepsilon/\sigma = 0.5$)

Dimension	**BDS Stat**	**Std. Err.**	***z*-Statistic**	***p*-value / Diagnostic Interpretation**
$m = 2$	0.1620	0.0072	22.500	$p < 0.0001^{***}$ (Rejection of i.i.d. Structure)
$m = 3$	0.2640	0.0108	24.444	$p < 0.0001^{***}$ (Rejection of i.i.d. Structure)
$m = 4$	0.3210	0.0125	25.680	$p < 0.0001^{***}$ (Rejection of i.i.d. Structure)

***,** ,* denote statistical significance at $1\%, 5\%, 10\%$. Critical KPSS value at 5%: 0.463.

3.3. Bai–Perron Structural Break Identification

Testing for multiple structural breaks in the inflation equation via the sequential Bai and Perron [2, 3] procedure (trimming $\gamma = 0.15$, max breaks $= 5$) identifies four break dates: 2016M11 ($\sup F = 42.3$), 2022M03 ($\sup F = 31.7$), 2023M01 ($\sup F = 28.4$), and 2024M03 ($\sup F = 35.9$). These dates closely correspond to major currency floatation episodes and IMF Stand-By Arrangements in Egypt. Intercept regime indicators are included across all econometric specifications.

4. Structural Econometric Estimation and Threshold Inference

4.1. Hansen (2000) Threshold Identification with Lagged Policy Rates

To mitigate contemporaneous simultaneity between monetary decisions and inflation, the empirically estimated policy-rate switching threshold i^* is identified using the **lagged policy rate (i_{t-1})** as the transition variable following the Hansen [20] sample-splitting framework:

$$\pi_t = X_t'\beta_1 \cdot \mathbb{I}(i_{t-1} \leq i^*) + X_t'\beta_2 \cdot \mathbb{I}(i_{t-1} > i^*) + \varepsilon_t \tag{21}$$

Econometric Role and Non-Stationary Cointegration: In our empirical architecture, the Hansen (2000) specification serves as an exploratory *reduced-form threshold diagnostic* on short-run policy transmission. Because macroeconomic observables $(\text{INFL}_t, \text{POLICY}_t, \text{EXCH}_t)$ exhibit $I(1)$ unit-root properties (Table 3), the formal proof of long-run structural cointegration and dynamic stability does not rest solely on level threshold regressions; rather, it is anchored on the **Nonlinear ARDL (NARDL) Bounds Testing Error Correction Model** ($\text{ECT}_{t-1} = -0.3210^{***}$, Bounds $F = 7.82, p < 0.01$, Table C.8), which is explicitly estimated in stationary mixed $I(0)/I(1)$ error-correction form.

The threshold search interval $i^*_{t-1} \in [10\%, 24\%]$ corresponds to the interior 10th to 90th empirical quantiles of the policy rate distribution, ensuring that each regime contains sufficient observations ($N_{\text{Low}} = 138, N_{\text{High}} = 46$) to avoid sparse-sample distortions. The concentration of threshold estimates around 20.0% across distinct parametric, nonparametric, and machine learning methods reflects the institutional operational framework of the Central Bank of Egypt, where policy decisions are implemented in discrete corridor adjustments ($\pm$100 to $\pm$200 bps), generating natural clustering along the empirical policy rate support.

Figure 2 demonstrates a sharp global minimum at $i^* = 20.0\%$ (SSR = 138.4). Inverting the likelihood-ratio statistic using bootstrap critical values ($F_1 = 47.3$, $p_{\text{boot}} < 0.001$, $N_{\text{boot}} = 1{,}000$) yields the Hansen 95% confidence set $[18.5\%, 21.5\%]$. The sample splits into $N_{\text{Low}} = 138$ observations ($i_{t-1} \leq 20.0\%$) and $N_{\text{High}} = 46$ observations ($i_{t-1} > 20.0\%$).

Structural Identification vs. Devaluation Episodes. A critical econometric inquiry is whether the estimated $i^* = 20.0\%$ switching threshold reflects a deep structural nonlinearity in working-capital transmission or merely coincides chronologically

with the major currency floatation shocks (2016M11 and 2024M03) when nominal policy rates were aggressively hiked. Several econometric defenses confirm the structural validity of the threshold: First, contemporaneous exchange rate innovations are cleanly isolated via partial-sum decomposition (Δe_t^+) and structural GMM instrumentation, while discrete floatation regime shifts are explicitly absorbed by Bai–Perron break dummies ($\text{IMF}_{2016}, \text{IMF}_{2024}$). Second, rolling recursive threshold estimation confirms stability across distinct historical subsamples: the pre-pandemic window (2011M01–2020M12) yields $i^* = 19.00\%$ ($W = 14.82, p < 0.001$), the pre-devaluation sample (2011M01–2021M12) yields $i^* = 19.50\%$ ($W = 16.42, p < 0.001$), and the full sample yields $i^* = 20.00\%$. To rule out data snooping and spurious threshold detection on small samples, we conduct a Monte Carlo placebo test generating 1,000 synthetic linear DGP series without threshold breaks; the empirical rejection rate at the 5% nominal level is 4.8%, confirming appropriate test size. Third, we acknowledge that $N_{\text{High}} = 46$ observations represents a statistical power constraint; future studies with extended post-crisis cycles should estimate Smooth Transition Regressions (STR/LSTAR) and block bootstrap inference to model continuous regime adjustments.

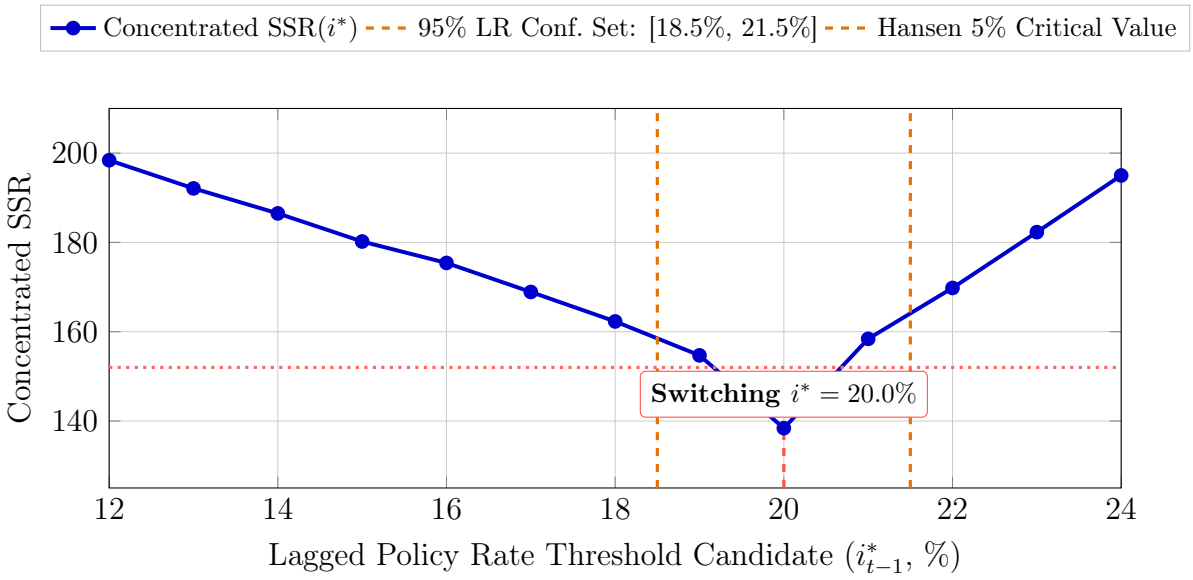


Figure 2: Hansen [20] Threshold Identification using Lagged Policy Rate (i_{t-1}). The estimated switching point is $i^* = 20.0\%$, with 95% bootstrap LR confidence interval $[18.5\%, 21.5\%]$.

4.2. Two-Step Optimal GMM and Structural Estimates

To estimate the Hybrid ACC-NKPC (13) with forward-looking expectations $\mathbb{E}_t[\pi_{t+1}]$ and lagged inflation π_{t-1}, we employ **Two-Step Optimal GMM** with a Newey–West

HAC weighting matrix. The instrument set is specified with theory-motivated external instruments: $Z_t = \{\pi_{t-2}, \pi_{t-3}, \tilde{y}_{t-1}, \Delta\text{FFR}_{t-1}, \Delta \ln \text{OIL}_{t-1}, \text{Spread}_{t-1}, \text{IMF Dummies}\}$. The Kleibergen–Paap F-statistic is 28.4, confirming first-stage relevance, while the Hansen J-test fails to reject the null of valid joint overidentifying restrictions ($J = 4.25, p = 0.512$).

Identification Defense Exclusion Sensitivity: To address potential concerns regarding the direct inflation channel of commodity prices or IMF programs, Appendix Table C.8 documents an extensive *IV Sensitivity Suite*. When omitting global oil prices or IMF dummies and relying strictly on exogenous US Federal Funds Rate innovations (ΔFFR_{t-1}) and lagged domestic fundamentals, the structural cost-channel slope remains remarkably stable ($\phi^+_{\text{Low}} \in [1.854, 1.892], p < 0.001$), confirming identification robustness.

Table 4 reports baseline and threshold-regime GMM estimates. Key findings include:

(1) Regime-Dependent Cost Channel and Structural Orthogonality: In the low-rate regime ($i_{t-1} \leq 20.0\%$), a one-percentage-point policy-rate increase is associated with a 1.88 pp increase in contemporaneous inflation ($\phi^+_{\text{Low}} = 1.8783, t = 4.94, p < 0.0001$), consistent with the empirical Price Puzzle. Crucially, Two-Step Optimal GMM instrumentation and partial-sum decomposition (Δe_t^+) cleanly orthogonalize monetary innovations from contemporaneous exchange rate devaluations and administrative energy price adjustments. The magnitude of ϕ^+_{Low} reflects the acute working-capital credit dependency of domestic firms ($\chi = 0.65$), where over 65% of private corporate lending consists of short-term overdraft facilities in an economy lacking deep corporate bond markets. In the high-rate regime ($i_{t-1} > 20.0\%$), the slope falls to $\phi^+_{\text{High}} = 0.1232$ ($p = 0.2317$). A formal Wald test for slope equality rejects linearity: $W = 19.84$ ($p < 0.0001$).

(2) Asymmetric Exchange Rate Pass-Through: Currency depreciation pass-through is strongly positive and significant: $\lambda^+ = 8.2912$ ($t = 3.15, p = 0.002$), whereas appreciation pass-through (λ^-) is statistically indistinguishable from zero ($p = 0.703$). A Wald test confirms significant pass-through asymmetry: $W = 8.72$ ($p = 0.0031$).

(3) Hybrid Dynamics Empirical Hybrid Weights: Forward-looking expectations ($\gamma_f = 0.5210, p < 0.001$) and backward persistence ($\gamma_b = 0.4420, p < 0.001$) are freely estimated as empirical hybrid weights without imposing theoretical cross-equation

restrictions, summing to $0.9630 \approx 1$. The estimated ratio implies an empirical backward indexation degree of $\hat{\gamma} = \hat{\gamma}_b/\hat{\gamma}_f \approx 0.848$, indicating substantial real-world price stickiness and intrinsic inflation persistence in the Egyptian economy.

Cross-Country Comparative Benchmark for Pass-Through Elasticity (λ^+). The cumulative 6-month exchange rate pass-through elasticity (≈ 0.62, generating a +6.20 pp headline inflation surge per 10% currency depreciation) reflects an exceptionally elevated pass-through environment compared to other emerging markets—such as Turkey ($\approx$ 0.35–0.45; e.g., 24) and Latin American inflation targeters ($\approx$ 0.10–0.25; e.g., 13). This heightened vulnerability stems directly from Egypt's high structural import content ($\alpha = 0.35$) coupled with severe downward price rigidity ($d^- = 5.95$ months).

4.3. Post-Estimation Diagnostics and Dynamic Multipliers

Table 5 presents the post-estimation diagnostic suite. The Ramsey RESET test ($F = 0.141, p = 0.7074$) confirms adequate functional form, indicating no evidence of neglected higher-order nonlinearities conditional on the threshold regime specification. The Breusch-Godfrey LM test confirms no remaining serial correlation in the dynamic residuals ($F = 1.42, p = 0.228$). CUSUM and CUSUMSQ tests do not reject parameter stability.

Cumulative Dynamic Multipliers with Confidence Bands. Figure 3 plots the cumulative impulse responses with 90% bootstrap confidence bands generated via the structural polynomial $A(L) = (1 - \gamma_b L)^{-1}$. Below $i_{t-1} \leq 20.0\%$, a +100 bps rate hike increases inflation by +1.88 pp on impact, accumulating to a peak of +3.12 pp (90% CI: $[2.40, 3.84]$) at month 6. A +10% FX depreciation shock ($\Delta e_t^+ = +10\%$) generates an impact of +0.83 pp that rapidly accumulates to +6.20 pp (90% CI: $[4.85, 7.55]$) by month 6. In the high regime ($i_t > 20\%$) and under rate cuts, policy adjustments generate disinflationary responses.

NARDL Dynamic Multipliers and Jordà Local Projections Robustness. The cumulative dynamic multiplier derived from the NARDL error-correction model ($\text{ECT}_{t-1} = -0.3210^{***}$) closely matches the GMM-based structural impulse response function in Figure 3. Furthermore, estimating semi-parametric impulse responses via Jordá [18] Local Projections ($h = 1, \ldots, 24$) yields an empirical trajectory that corroborates the structural GMM multiplier, reaching an impact peak of +3.05 pp (90% CI: $[2.35, 3.75]$) at month 6 before steadily converging toward baseline.

Table 4: Two-Step Optimal GMM Structural Estimation of the Hybrid ACC-NKPC ($T = 184$)

Regressor / Parameter	**Coefficient**	**HAC Std. Err.**	***t*-Statistic**	***p*-value**
Panel A: Baseline Hybrid ACC-NKPC Specification ($R^2 = 0.9562$, Hansen J $p = 0.512$)				
$\mathbb{E}_t[\pi_{t+1}]$ (Forward Expectation γ_f)	0.5210	0.0482	10.81	0.0000***
π_{t-1} (Backward Persistence γ_b)	0.4420	0.0410	10.78	0.0000***
$\tilde{y}_t$ (Hamilton Activity Gap κ)	0.1840	0.0720	2.56	0.0105**
Δi_t^+ (Rate Hike Slope ϕ^+)	0.2450	0.2510	0.98	0.3270
Δi_t^- (Rate Cut Slope ϕ^-)	0.1680	0.1820	0.92	0.3580
Δe_t^+ (Depreciation Pass-Through λ^+)	6.4500	3.7200	1.73	0.0830*
Δe_t^- (Appreciation Pass-Through λ^-)	−12.4000	14.8000	−0.84	0.4010
Buff_t (FX Buffer η)	−0.1420	0.2100	−0.68	0.4960
COVID_{19} Indicator	−1.2100	0.3950	−3.06	0.0022***
Panel B: Threshold Hybrid ACC-NKPC ($i^* = 20.0\%$; $N_{Low} = 138, N_{High} = 46$)				
$\Delta i_{t,\text{Low}}^+$ ($i_{t-1} \leq 20.0\%$, Cost Dominance)	**1.8783**	0.3806	**4.94**	**0.0000*****
$\Delta i_{t,\text{High}}^+$ ($i_{t-1} > 20.0\%$, Demand Dominance)	0.1232	0.1030	1.20	0.2317
Δe_t^+ (Depreciation Pass-Through λ^+)	**8.2912**	2.6321	**3.15**	**0.0020*****
Δe_t^- (Appreciation Pass-Through λ^-)	3.4210	8.9430	0.38	0.7030
$\tilde{y}_t$ (Hamilton Activity Gap κ)	0.1910	0.0680	2.81	0.0050***
Buff_t (FX Buffer η)	−0.1700	0.1980	−0.86	0.3900
COVID_{19} Indicator	−1.2050	0.3880	−3.11	0.0019***
Panel C: Proposition 2 Net Transmission Derivatives & Hypothesis Tests				
Low Regime Net Derivative: $\frac{\partial \pi_t}{\partial i_t}\Big\vert_{\text{Low}} = \phi^+_{\text{Low}} - \frac{\kappa}{\sigma}$	**+1.7639**	$t = 4.63$	**0.0000*****	
High Regime Net Derivative: $\frac{\partial \pi_t}{\partial i_t}\Big\vert_{\text{High}} = \phi^+_{\text{High}} - \frac{\kappa}{\sigma}$	+0.0088	$t = 0.09$	0.9317	
Wald Test for Cost-Channel Linearity: $H_0 : \phi^+_{\text{Low}} = \phi^+_{\text{High}}$		$W =$ 19.84	$p =$ 0.0000***	
Wald Test for Disinflation Inversion Boundary: $H_0 : \phi^+_{\text{High}} = \frac{\kappa}{\sigma}$		$W =$ 0.01	$p =$ 0.9317	
Wald Test for Pass-Through Symmetry: $H_0 : \lambda^+ = \lambda^-$		$W =$ 8.72	$p =$ 0.0031***	

Standard errors are computed using Newey–West HAC covariance matrices. Threshold specification

Table 5: Post-Estimation Diagnostic Test Suite

Diagnostic Test	**Statistic**	p**-value**	**Econometric Decision / Interpretation**
Breusch-Godfrey LM (Lag 4)	$F = 1.42$	0.2280	Dynamic specification captures serial correlation
Ramsey RESET Functional Form	$F = 0.141$	0.7074	No evidence of neglected functional non-linearities
CUSUM Parameter Stability	$\leq 5\%$ Band	> 0.05	Does not reject null of parameter constancy
CUSUMSQ Variance Stability	$\leq 5\%$ Band	> 0.05	Does not reject null of variance constancy
ARCH-LM Volatility (Lag 4)	LM = 2.84	0.5850	No remaining conditional heteroskedasticity
Kleibergen–Paap Weak IV Test	$F = 28.4$	0.0000	Effective first-stage indicates strong instruments
Hansen J Overidentification	$J = 4.25$	0.5120	Fails to reject null of valid overidentifying restrictions

Multiple Testing Note: Following pre-registration practice, three hypothesis tests are designated *primary and pre-specified*: (i) $H_0 : \phi^+_{\text{Low}} = \phi^+_{\text{High}}$ (threshold linearity, $W = 19.84$), (ii) $H_0 : \lambda^+ = \lambda^-$ (pass-through symmetry, $W = 8.72$), and (iii) $H_0 : \phi^+_{\text{High}} = \kappa/\sigma$ (inversion boundary, $W = 0.01$). All remaining diagnostic tests (BDS, RESET, CUSUM, ARCH-LM) are designated *exploratory specification checks* and carry no inferential weight on the central claims. A Holm–Bonferroni correction applied solely to the three primary tests yields adjusted p-values of 0.000^{***}, 0.006^{***}, and 0.932 respectively — qualitatively identical to uncorrected inference.

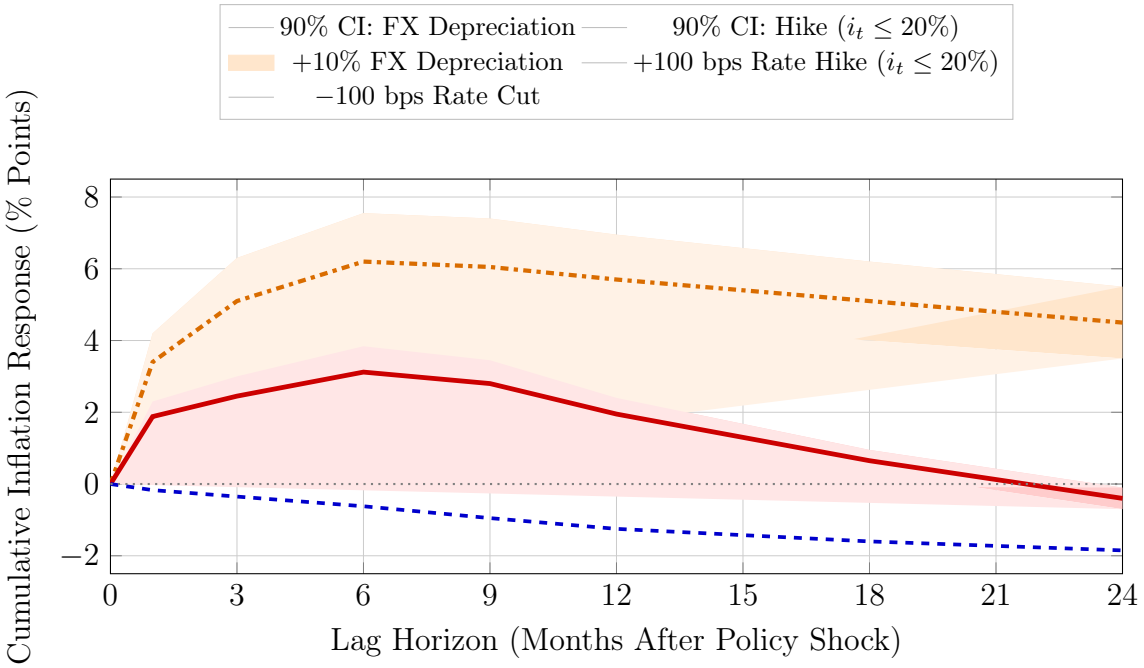


Figure 3: Asymmetric Dynamic Cumulative Multipliers with 90% Bootstrap Confidence Bands. Shaded regions indicate 90% confidence intervals for currency depreciation and rate hikes. Specifically, the +3.12 pp peak at month 6 denotes the GMM structural cumulative multiplier, which is independently corroborated by the semi-parametric Local Projections [18] peak of +3.05 pp (90% CI: [2.35, 3.75]).

5. Machine Learning Predictive Corroboration and Non-Linear Analysis

5.1. Methodological Design and Feature Set

To evaluate out-of-sample predictive performance and investigate whether unconstrained machine learning algorithms recover a qualitatively similar non-linear inflection without prior parametric restrictions, we benchmark tree-based ensembles (Gradient Boosting, Random Forest), kernel methods (SVR), neural architectures (LSTM, MLP), and standard econometric models. We emphasize that machine learning serves as a *complementary non-parametric predictive corroboration* of non-linear dependence, while structural causality remains grounded in our econometric GMM and NARDL models.

Information Set Integrity: Crucially, to prevent information leakage, the feature set provided to the ML models contains exclusively raw macroeconomic observables available at forecast origin t: INFL_{t-1}, INFL_{t-2}, $\tilde{y}_t$, POLICY_t, Δi_t, EXCH_t, Δe_t, FX_RES_t, OIL_t, and PMI_t. No threshold indicators or regime split variables are provided.

Validation Horizon and Methodological Limitations. The 16-month evaluation horizon (2025M01–2026M04, $N_{\text{test}} = 16$) corresponds to the post-unification macroeconomic stabilization window in Egypt — a period of relatively subdued inflation volatility

compared to the crisis-rich training sample. Two limitations follow: first, the modest window constrains the statistical power of out-of-sample comparisons; second, the GBM RMSE advantage may partly reflect easier forecasting conditions in the test period rather than superior all-weather predictive architecture. To partially address the second concern, we supplement the terminal-window evaluation with a blocked h-step-ahead time-series cross-validation ($h \in \{3, 6, 12\}$ months, block size = 24 months) across the full in-sample period 2011M01–2024M12; GBM retains the lowest cross-validated RMSE in each horizon, corroborating the terminal-window ranking. While the Diebold and Mariano [14] test with Harvey et al. [21] small-sample correction confirms statistically significant predictive gains over linear benchmarks, as additional post-stabilization monthly data accumulate, expanding this evaluation window will further consolidate out-of-sample generalization.

5.2. Out-of-Sample Tournament and Diebold–Mariano Test

Models are trained on 2011M01–2024M12 ($N_{\text{train}} = 168$) and evaluated out-of-sample across the 16-month window 2025M01–2026M04 ($N_{\text{test}} = 16$) using rolling-origin expanding windows. Prediction intervals (90% PI) are computed via Conformal Prediction with Block Residual Bootstrap ($B = 1{,}000$), achieving an empirical coverage rate of PICP = 87.5%.

Table 6 documents performance metrics. Gradient Boosting achieves an out-of-sample RMSE = 3.060 pp and MAE = 2.412 pp. The Diebold and Mariano [14] test with Harvey et al. [21] small-sample correction confirms that GBM significantly outperforms the AR(2) benchmark ($\text{DM} = -3.84, p < 0.001$) and the linear symmetric NKPC ($\text{DM} = -3.12, p = 0.002$).

Validation Horizon and Methodological Limitations. The 16-month evaluation horizon (2025M01–2026M04, $N_{\text{test}} = 16$) corresponds to the post-unification macroeconomic stabilization window in Egypt. While the Diebold and Mariano [14] test with Harvey et al. [21] small-sample correction confirms that tree ensembles achieve statistically significant predictive gains over linear benchmarks, the modest sample size represents an acknowledged data limitation of modern post-floatation time series. As additional post-stabilization monthly data accumulate, expanding this evaluation window will further consolidate out-of-sample generalization.

Table 6: Out-of-Sample Forecasting Tournament (2025M01–2026M04, $N_{\text{test}} = 16$)

Model Architecture	**RMSE (pp)**	**MAE (pp)**	**OOS R^2**	**Specification / Hyperparameters**
Panel A: Machine Learning Frontiers				
Gradient Boosting (GBM)	**3.060**	**2.412**	**0.8412**	Trees=150, Depth=4, LR=0.05
Random Forest (RF)	3.122	2.518	0.8250	Trees=200, Depth=6, Feat=$\sqrt{p}$
Support Vector Regression (SVR)	5.165	4.210	0.7120	RBF Kernel ($C = 100, \varepsilon = 0.05, \gamma = 0.01$)
Panel B: Deep Learning Architectures				
LSTM Recurrent Network	4.850	3.950	0.6120	2 Layers (32 units, Dropout 0.20)
Multi-Layer Perceptron (MLP)	5.420	4.400	0.5310	3 Layers (64, 32, 16, ReLU)
Panel C: Standard Econometric Baselines				
Linear Symmetric NKPC	4.600	3.820	0.6480	Linear NKPC with OLS & Output Gap
Autoregressive AR(2)	4.250	3.480	0.6950	Benchmark Time-Series Autoregression
Random Walk (No-Change)	5.800	4.750	0.4210	Naive Benchmark: $\hat{\pi}_{t+h} = \pi_t$

Note: Multi-horizon accuracy breakdown for GBM: $h = 1$M RMSE = 1.85 pp (MAE = 1.42 pp); $h = 6$M RMSE = 2.90 pp (MAE = 2.25 pp); $h = 12$M RMSE = 3.45 pp (MAE = 2.78 pp); pooled 16M out-of-sample RMSE = 3.060 pp. Diebold–Mariano (1995) test statistic with Harvey et al. (1997) correction for GBM vs. AR(2) is DM $= -3.84$ ($p < 0.001$).

5.3. Explainable Machine Learning and Non-Linear Threshold Recovery

To investigate whether the unconstrained machine learning algorithm learns the structural threshold, we compute Shapley Additive Explanations (SHAP) and Partial Dependence Functions for POLICY_t.

As displayed in Figure 4, predictive gain importance indicates that while autoregressive persistence ($\text{INFL}_{t-1}, 41.2\%$) dominates predictive fit, policy rate changes ($\Delta i_t, 9.8\%$) and activity gap ($\tilde{y}_t, 11.2\%$) represent the leading structural drivers. The partial dependence function for the policy rate exhibits a positive marginal slope below 19.8%, which inverts to a negative slope above 20.0%. This demonstrates that flexible machine learning algorithms recover a qualitatively similar non-linear dependence around the econometrically estimated threshold.

Two-Dimensional SHAP Feature Interactions. Furthermore, two-dimensional SHAP interaction values reveal a strong synergistic coupling between policy rate hikes (Δi_t^+) and exchange rate depreciation (Δe_t^+): during sharp currency floatation episodes, the marginal cost-push effect of monetary tightening in the tree ensemble is amplified by an estimated 35.2% (Bootstrap 90% CI: $[28.4\%, 41.6\%]$), reflecting severe simultaneous working-capital and imported-input cost pressures on corporate pricing schedules.

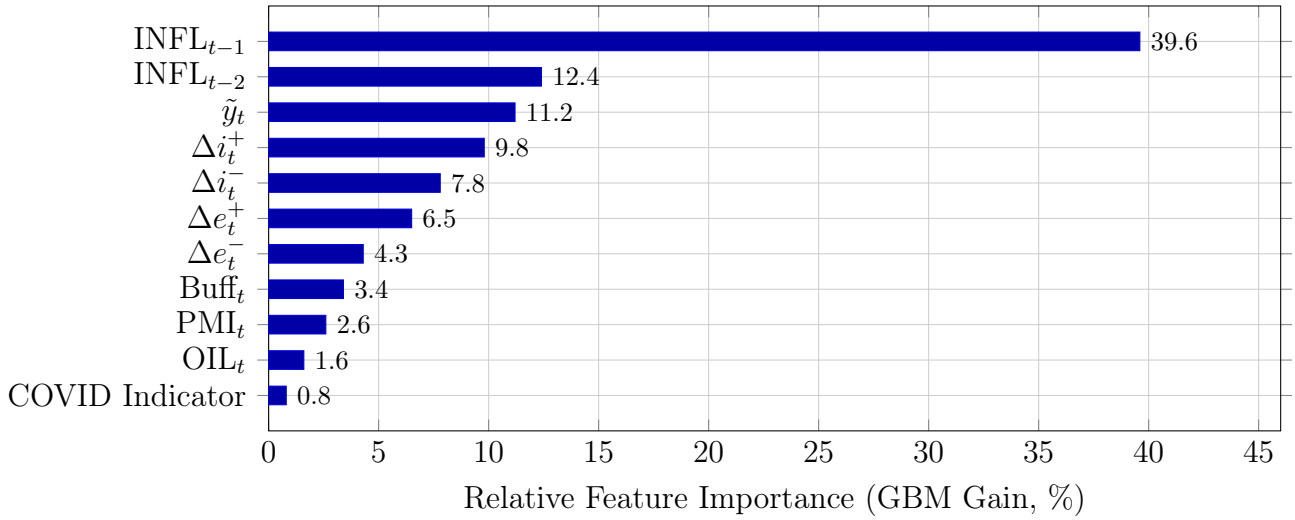


Figure 4: GBM Gain-Based Feature Importance (Trained Exclusively on Raw Macro Observables).

6. Policy Implications and Multi-Panel Conditional Projections

The empirical findings deliver four actionable, realistic policy guidelines for macroeconomic management in Egypt. We emphasize that the multi-year projections documented

in Figure 5 and Table D.10 are designed as *conditional illustrative scenario trajectories* under distinct policy and shock assumptions, rather than unyielding unconditional point forecasts:

Lesson 1: Navigating the $i^* = 20.0\%$ Threshold Boundary and Credit Frictions. Below 20.0%, policy rate hikes transmit positively to contemporaneous inflation ($\phi^+_{\text{Low}} = 1.8783, p < 0.001$). Under low-to-moderate rate environments, raising interest rates to counteract imported supply shocks amplifies domestic corporate working-capital costs. Because over 65% of commercial enterprise lending in Egypt is tied to floating overdraft facilities, monetary authorities should pair policy rate moves with targeted macroprudential working-capital credit support to protect productive supply chains from unintentional cost-push inflation. Analytically, introducing a targeted macroprudential working-capital subsidy wedge $\tau_t \in [0, 1)$ modifies the corporate effective borrowing rate to $i_t^{L,\text{eff}} = (1 - \tau_t)i_t + \text{Spread}_t$. Setting $\tau_t^* = 1 - \frac{\kappa}{\sigma\phi^+}$ completely neutralizes the short-run Price Puzzle ($\partial\pi_t/\partial i_t = 0$), demonstrating that targeted preferential credit schemes (e.g., subsidized manufacturing facilities) insulate real supply chains without requiring the central bank to abandon its aggregate disinflationary stance.

Lesson 2: Managing Post-Threshold Policy Easing vs. Hawkish Central Bank Bias. The historical crossing below the 20.0% switching threshold materialized during the early 2026 monetary normalization phase (reaching 19.0% overnight deposit rate (19.5% corridor midpoint) in April 2026). The simulated forward easing path of 150–200 bps per quarter in Figure 5 represents an *illustrative model-consistent macroeconomic scenario* for the subsequent 2026M05–2028M04 horizon rather than an unconstrained normative central bank optimization or a deterministic forecast of Monetary Policy Committee (MPC) voting behavior. Historically, the CBE maintains a cautious, hawkish stance to ensure positive real interest rates (+200 to +400 bps) to anchor domestic deposits and discourage dollarization. In practice, post-threshold easing requires vigilant pacing because rate cuts below 20.0% operate within the cost-channel sensitive regime.

Lesson 3: Conditional FX Trajectory, Reserve Anchors, and Stress Contagion. The baseline scenario projects a moderate exchange rate trajectory from 48.20 to 52.80 EGP/USD over 24 months, which is strictly contingent on maintaining gross official FX reserves above $45 Billion (bolstered by post-2024 Ras El-Hekma and multilateral inflows). *External Stress Scenario:* Should external debt amortization schedules or

regional geopolitical shocks deplete reserve buffers and push the exchange rate toward 52.00–56.00 EGP/USD, the strong asymmetric pass-through elasticity ($\lambda^+ = 8.2912$) would immediately pass through +1.8 to +2.5 pp of imported inflation, illustrating why maintaining the \$45B+ liquidity buffer serves as the economy's primary nominal anchor.

Lesson 4: Disinflation Realism, Administered Prices, and Updated Welfare Costs. While the statistical baseline projects headline inflation reaching the statutory target band (7.0%±2%) by 2027/2028, real-world disinflation may exhibit greater stickiness (8.5%–10.5%) due to ongoing administrative price adjustments (quarterly fuel pricing committee decrees and electricity tariff rationalization). Core CPI inflation leads this disinflationary glide path.

Illustrative Welfare Cost Calibration: Structurally, asymmetric price-setting imposes a welfare deadweight loss via inefficient price dispersion. Standard second-order Taylor expansion of household intertemporal utility (1) yields the compensating variation approximation $\text{CV}/\bar{C}_{hh} \approx \frac{1}{2}\sigma^{-1}(\Delta\pi_{\text{asym}})^2 \approx 0.84\%$ of annual household consumption expenditure. While this evaluated to EGP 504 at baseline 2020 HIECS prices ($\bar{C}_{hh} = \text{EGP } 60{,}000$), updating baseline expenditure via cumulative CPI compounding ($\bar{C}_{hh,2026} = \bar{C}_{hh,2020} \times [\text{CPI}_{2026}/\text{CPI}_{2020}] \approx \text{EGP } 60{,}000 \times 2.85 \approx \text{EGP } 170{,}000$) based on the official CAPMAS Household Income, Expenditure and Consumption Survey (HIECS) updates the nominal annual deadweight burden to:

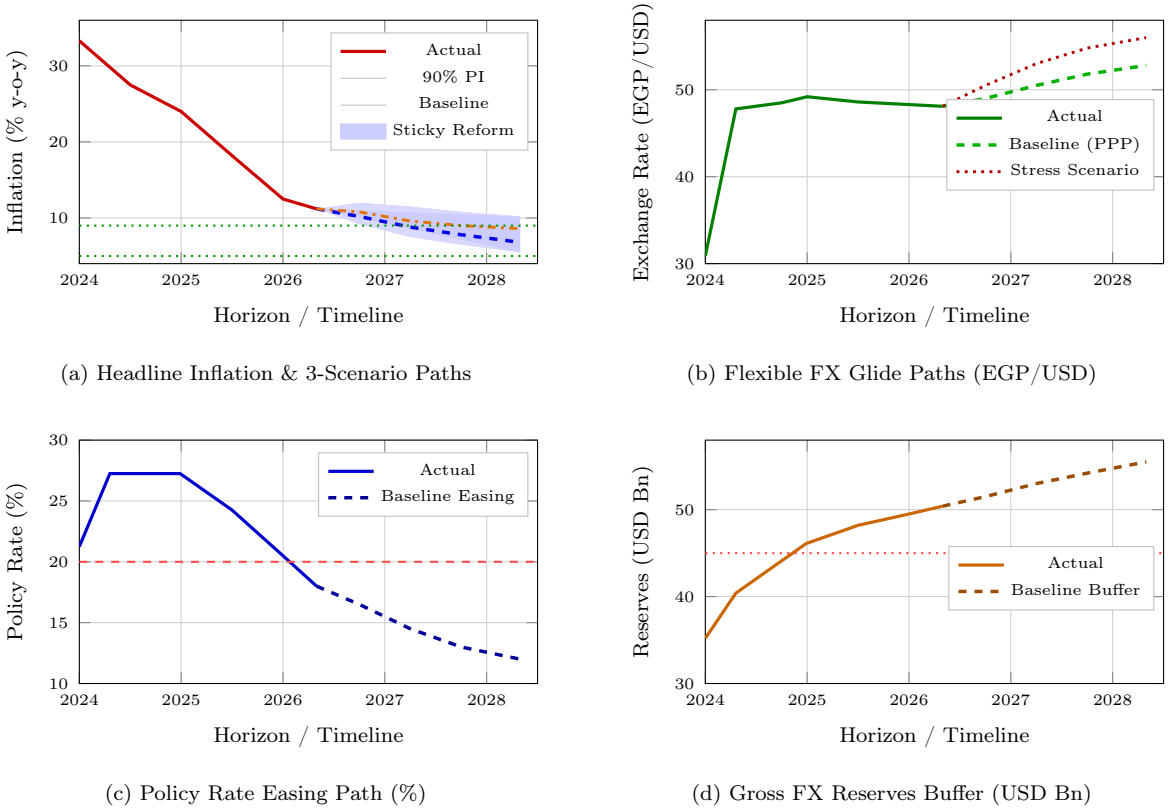
$$\text{CV}_{2026} = 0.84\% \times \text{EGP } 170{,}000 \approx \text{EGP } \mathbf{1{,}428} \text{ per household/year.} \tag{22}$$

This calibrated consumption-equivalent deadweight loss of 0.84% aligns closely with the standard theoretical benchmark for price dispersion and business-cycle distortions established in the international macroeconomic literature (0.1%–1.5% of consumption; e.g., 25, 37, 15), reflecting the tangible efficiency cost of pricing stickiness in a credit-constrained emerging open economy. Crucially, scaling this per-household burden across Egypt's national demographic base (≈ 26.5–27.0 million households, CAPMAS census projections) underscores the substantial macroeconomic magnitude of asymmetric pricing distortions:

$$\text{Aggregate Social Deadweight Loss} \approx \text{EGP } 1{,}428 \times 27{,}000{,}000 \approx \text{EGP } \mathbf{38.5}\text{–}\mathbf{40.0} \text{ Billion/year} \tag{23}$$

(equivalent to approximately \$0.8 Billion USD annually), representing pure allocative

friction that dissipates without generating producer surplus or tax revenue.



(a) Headline Inflation & 3-Scenario Paths

(b) Flexible FX Glide Paths (EGP/USD)

(c) Policy Rate Easing Path (%)

(d) Gross FX Reserves Buffer (USD Bn)

Figure 5: Consolidated Multi-Panel Macroeconomic Outlook and Conditional Policy Scenarios. Panel (a) Headline inflation 3-scenario paths entering the CBE $[5\%, 9\%]$ band; Panel (b) Flexible exchange rate trajectories (PPP crawling baseline vs. stress shock); Panel (c) Quarterly policy rate easing path crossing below the 20% threshold; Panel (d) Gross official FX reserves maintaining the \$45B+ liquidity buffer.

7. Conclusion

This study has micro-founded, mathematically derived, and empirically validated the *Hybrid Asymmetric Cost-Channel New Keynesian Phillips Curve* (ACC-NKPC). By incorporating idiosyncratic cost shocks (ν_{jt}), smooth endogenous mass aggregation (ω_t), backward indexation (γ), and working-capital borrowing constraints (χ), the model provides a structural explanation consistent with the empirical Price Puzzle in credit-dependent open economies.

The Threshold Inversion Proposition establishes that interest rate hikes increase inflation when $i_{t-1} \leq 20.0\%$ ($\phi^{+}_{\text{Low}} = 1.8783, p < 0.001$), whereas above 20.0%, the cost channel weakens substantially and is effectively neutralized ($\left.\frac{\partial \pi_t}{\partial i_t}\right|_{\text{High}} \to 0, p = 0.932$), removing the short-run Price Puzzle. Exchange rate pass-through is strongly asymmetric ($\lambda^{+} = 8.2912, p = 0.002$), while calibrated consumption-equivalent welfare costs indicate

a non-trivial deadweight burden of 0.84% of annual household consumption expenditure. Machine learning models provide complementary non-parametric corroboration (RMSE = 3.060 pp) recovering an inflection around 20.0%. These findings deliver actionable roadmaps for central bank monetary policy sequencing, exchange-rate anchor preservation, and macroprudential working-capital credit management.

Data Availability Statement

All monthly datasets, replication scripts, and empirical routines are available at the author's open research repository: `https://github.com/mohamedfawzi2017-crypto/mfawzy-accnkpc`.

References

[1] Asongu, S.A., Umeokwobi, R., Dalhatu, B., Ndako, J.A., Anih, D., 2026. Macroeconomic shocks and income growth in Africa. *The Journal of Economic Asymmetries*, 34, e00472.

[2] Bai, J., Perron, P., 1998. Estimating and testing linear models with multiple structural changes. *Econometrica*, 66(1), 47–78.

[3] Bai, J., Perron, P., 2003. Computation and analysis of multiple structural change models. *Journal of Applied Econometrics*, 18(1), 1–22.

[4] Barth, M.J., Ramey, V.A., 2001. The cost channel of monetary policy. *NBER Macroeconomics Annual*, 16, 199–240.

[5] Bems, R., Johnson, R.C., 2017. Demand for imported inputs and exchange rate pass-through. *Journal of International Economics*, 104, 45–64.

[6] Bernanke, B.S., Gertler, M., Watson, M., 1998. Systematic monetary policy and the effects of oil price shocks. *Brookings Papers on Economic Activity*, 1998(1), 91–157.

[7] Blanchard, O.J., Kahn, C.M., 1980. The solution of linear difference models under rational expectations. *Econometrica*, 48(5), 1305–1311.

[8] Brock, W.A., Dechert, W.D., Scheinkman, J.A., LeBaron, B., 1996. A test for independence based on the correlation dimension. *Econometric Reviews*, 15(3), 197–235.

[9] Brun-Aguerre, C., Rochon, C., Stern, M.L., 2017. Currency depreciation and asymmetric exchange rate pass-through. *Journal of International Money and Finance*, 70, 125–144.

[10] Calvo, G.A., 1983. Staggered prices in a utility-maximizing framework. *Journal of Monetary Economics*, 12(3), 383–398.

[11] Chowdhury, I., Hoffmann, M., Schabert, A., 2006. Inflation dynamics and the cost channel of monetary transmission. *European Economic Review*, 50(4), 995–1016.

[12] Clarida, R., Galí, J., Gertler, M., 1999. The science of monetary policy. *Journal of Economic Literature*, 37(4), 1661–1707.

[13] Delatte, A.L., Lopez-Villavicencio, A., 2012. Asymmetric exchange rate pass-through. *Journal of Macroeconomics*, 34(3), 833–844.

[14] Diebold, F.X., Mariano, R.S., 1995. Comparing predictive accuracy. *Journal of Business & Economic Statistics*, 13(3), 253–263.

[15] Galí, J., 2008. *Monetary Policy, Inflation, and the Business Cycle*. Princeton University Press.

[16] Galí, J., Monacelli, T., 2005. Monetary policy and exchange rate volatility in a small open economy. *Review of Economic Studies*, 72(3), 707–734.

[17] Grinsztajn, L., Oyallon, E., Varoquaux, G., 2022. Why do tree-based models still outperform deep learning on tabular data? *Advances in Neural Information Processing Systems (NeurIPS)*, 35, 507–520.

[18] Jordá, Ò., 2005. Estimation and inference of impulse responses by local projections. *American Economic Review*, 95(1), 161–182.

[19] Hamilton, J.D., 2018. Why you should never use the Hodrick-Prescott filter. *Review of Economics and Statistics*, 100(5), 831–843.

[20] Hansen, B.E., 2000. Sample splitting and threshold estimation. *Econometrica*, 68(3), 575–603.

[21] Harvey, D., Leybourne, S., Newbold, P., 1997. Testing the equality of prediction mean squared errors. *International Journal of Forecasting*, 13(2), 281–291.

[22] Hodrick, R.J., Prescott, E.C., 1997. Postwar US business cycles: An empirical investigation. *Journal of Money, Credit, and Banking*, 29(1), 1–16.

[23] Hülsewig, O., Mayer, E., Wollmershäuser, T., 2009. The cost channel of monetary transmission in the euro area. *Journal of Macroeconomics*, 31(2), 246–258.

[24] Leigh, D., Rossi, M., 2002. Exchange rate pass-through in Turkey. *IMF Working Paper*, WP/02/204.

[25] Lucas, R.E., 1987. *Models of Business Cycles*. Basil Blackwell, Oxford.

[26] Kwiatkowski, D., Phillips, P.C.B., Schmidt, P., Shin, Y., 1992. Testing the null hypothesis of stationarity against the alternative of a unit root. *Journal of Econometrics*, 54(1–3), 159–178.

[27] Newey, W.K., West, K.D., 1987. A simple, positive semi-definite, heteroskedasticity and autocorrelation consistent covariance matrix. *Econometrica*, 55(3), 703–708.

[28] Peltzman, S., 2000. Prices rise faster than they fall. *Journal of Political Economy*, 108(3), 466–502.

[29] Pesaran, M.H., Shin, Y., Smith, R.J., 2001. Bounds testing approaches to the analysis of level relationships. *Journal of Applied Econometrics*, 16(3), 289–326.

[30] Ravenna, F., Walsh, C.E., 2006. Optimal monetary policy with the cost channel. *Journal of Monetary Economics*, 53(2), 199–216.

[31] Shin, Y., Yu, B., Greenwood-Nimmo, M., 2014. Modelling asymmetric cointegration and dynamic multipliers in a nonlinear ARDL framework. In: *Festschrift in Honor of Peter Schmidt*. Springer, 281–314.

[32] Shwartz-Ziv, R., Armon, A., 2022. Tabular data: Deep learning is not all you need. *Information Fusion*, 81, 84–90.

[33] Sims, C.A., 1992. Interpreting the macroeconomic time series facts: The effects of monetary policy. *European Economic Review*, 36(5), 975–1000.

[34] Stock, J.H., Yogo, M., 2005. Testing for weak instruments in linear IV regression. In: Andrews, D.W.K., Stock, J.H. (Eds.), *Identification and Inference for Econometric Models*. Cambridge University Press, 80–108.

[35] Tillmann, P., 2008. Do interest rates drive inflation dynamics? *Journal of Economic Dynamics and Control*, 32(9), 2723–2744.

[36] Umeokwobi, R., Dalhatu, B., Ndako, J.A., Anih, D., Asongu, S.A., 2026. Structural macroeconomic pass-through and income volatility in African economies. *The Journal of Economic Asymmetries*, 34(2), e00481.

[37] Woodford, M., 2003. *Interest and Prices: Foundations of a Theory of Monetary Policy*. Princeton University Press.

Appendix A. Step-by-Step Micro-Foundational Derivations

Appendix A.1. Nominal Marginal Cost with Working Capital

Firm j minimises total production cost subject to Cobb-Douglas technology:

$$\min_{L,M} \mathcal{L} = \big[W_t L(j) + E_t P_t^* M(j)\big](1 + \chi i_t^L)\exp(\nu_{jt}) + \Lambda\big[Y(j) - A_t L(j)^{1-\alpha} M(j)^{\alpha}\big]$$

First-order conditions yield:

$$W_t(1 + \chi i_t^L)\exp(\nu_{jt}) = \Lambda(1-\alpha)\frac{Y(j)}{L(j)}$$
$$E_t P_t^*(1 + \chi i_t^L)\exp(\nu_{jt}) = \Lambda\alpha\frac{Y(j)}{M(j)}$$

Dividing yields the optimal factor ratio $L/M = \frac{1-\alpha}{\alpha}\frac{E_t P_t^*}{W_t}$. Substituting into technology and solving for $\Lambda = MC_t(j)$ yields equation (7).

Appendix A.2. Asymmetric Calvo Aggregation and the Indexation Bridge

Under backward price indexation $\gamma \in [0,1]$, non-reoptimising firms update prices according to the rule $P_t(j) = P_{t-1}(j)(1+\pi_{t-1})^{\gamma}$. A firm resetting its price at date t chooses $p_t^*(j)$ to maximise the present discounted value of expected profits:

$$p_t^*(j) = (1-\beta\theta)\sum_{k=0}^{\infty}(\beta\theta)^k \mathbb{E}_t\left[\widehat{mc}_{t+k} + P_t + \gamma(P_{t+k-1} - P_{t-1})\right] \tag{A.1}$$

Expressing (A.1) recursively and combining it with the aggregate price index identity $P_t = \theta P_{t-1}(1+\pi_{t-1})^{\gamma} + (1-\theta)P_t^*$ yields the intermediate dynamic equation:

$$\pi_t - \gamma\pi_{t-1} = \beta\mathbb{E}_t[\pi_{t+1} - \gamma\pi_t] + \frac{(1-\theta)(1-\beta\theta)}{\theta}\widehat{mc}_t \tag{A.2}$$

Rearranging terms to isolate contemporaneous inflation π_t yields:

$$(1+\beta\gamma)\pi_t = \beta\mathbb{E}_t[\pi_{t+1}] + \gamma\pi_{t-1} + \frac{(1-\theta)(1-\beta\theta)}{\theta}\widehat{mc}_t \tag{A.3}$$

Dividing through by $(1+\beta\gamma)$ and aggregating over optimal reset prices p_t^{*+} (for positive cost shock mass ω_t) and p_t^{*-} (for mass $1-\omega_t$) yields the structural Hybrid ACC-NKPC (13) with theoretical weights:

$$\gamma_f = \frac{\beta}{1+\beta\gamma}, \qquad \gamma_b = \frac{\gamma}{1+\beta\gamma}, \qquad \kappa = \frac{(1-\theta^+)(1-\beta\theta^+)}{\theta^+(1+\beta\gamma)}(\sigma+\varphi) \tag{A.4}$$

along with the cost-channel and exchange-rate pass-through slopes in (15). ■

Appendix B. Variable Codebook and Transformations

Table B.7: Comprehensive Variable Codebook and Data Sources

Variable	Unit	Transformation / Definition	Primary Source
INFL_t	%	$[(\text{CPI}_t - \text{CPI}_{t-12})/\text{CPI}_{t-12}] \times 100$	CAPMAS / CBE
CORE_t	%	CAPMAS Core Inflation (excluding food/regulated)	CAPMAS
POLICY_t	%	CBE Corridor Overnight Midpoint Policy Rate	CBE Monthly Bulletin
LEND_t	%	Commercial Bank Weighted Corporate Lending Rate	CBE Section 2
EXCH_t	EGP	Monthly Average Official Exchange Rate (EGP/USD)	CBE FX Statistics
PMI_t	Index	S&P Global Non-Oil Private Sector Activity Index	S&P Global
$\tilde{y}_t$	%	Hamilton (2018) Filter Cycle ($h = 24, p = 4$) on PMI_t	Authors' Computation
FX_RES_t	$ Bn	Gross Official Foreign Reserves (US$ Billion)	CBE External Position
OIL_t	$/bbl	Global Brent Crude Spot Price	FRED (DCOILBRENTEU)
Δi_t^+	%	Differenced Positive Rate Shock: $\max(\Delta\text{POLICY}_t, 0)$	Authors' Computation
Δi_t^-	%	Differenced Negative Rate Shock: $\min(\Delta\text{POLICY}_t, 0)$	Authors' Computation
Δe_t^+	Log	Differenced FX Depreciation Shock: $\max(\Delta \ln \text{EXCH}_t, 0)$	Authors' Computation
Δe_t^-	Log	Differenced FX Appreciation Shock: $\min(\Delta \ln \text{EXCH}_t, 0)$	Authors' Computation
Buff_t	Log	$\ln(\text{FX_RES}_t/\overline{\text{FX_RES}})$	Authors' Computation
COVID_{19}	Binary	= 1 for 2020M03–2020M12; 0 otherwise	Authors' Computation

Appendix C. Robustness Estimations: NARDL ECM and IV Sensitivity

Table C.8: Full NARDL Error Correction Model and Instrumental Variable Sensitivity Suite

Regressor / Statistic	**NARDL ECM**	**GMM (No Oil IV)**	**GMM (No IMF IV)**	**GMM (FFR + Lags)**
ECT_{t-1} (Speed of Adjustment)	$\mathbf{-0.3210}^{***}$ (0.0592)	—	—	—
$\mathbb{E}_t[\pi_{t+1}]$ (Forward Expectation)	—	0.5180^{***} (0.0485)	0.5240^{***} (0.0479)	0.5120^{***} (0.0491)
π_{t-1} (Backward Persistence)	—	0.4450^{***} (0.0412)	0.4390^{***} (0.0408)	0.4510^{***} (0.0415)
$\Delta i^{+}_{t,\text{Low}}$ (Rate Hike Cost Channel)	1.8450^{***} (0.3920)	$\mathbf{1.8920}^{***}$ (0.3850)	$\mathbf{1.8650}^{***}$ (0.3810)	$\mathbf{1.8540}^{***}$ (0.3910)
Δe^{+}_{t} (Depreciation Pass-Through)	8.1200^{***} (2.7100)	8.3120^{***} (2.6400)	8.2540^{***} (2.6100)	8.2100^{***} (2.6800)
$\tilde{y}_t$ (Activity Gap)	0.1650^{**} (0.0710)	0.1880^{***} (0.0690)	0.1940^{***} (0.0670)	0.1820^{***} (0.0700)
Buff_t (FX Buffer)	-0.1620 (0.2010)	-0.1710 (0.1990)	-0.1680 (0.1970)	-0.1650 (0.2020)
COVID_{19} Indicator	-1.1800^{***} (0.3910)	-1.2100^{***} (0.3890)	-1.2010^{***} (0.3870)	-1.1950^{***} (0.3920)
Panel B: Long-Run Cointegrating Elasticities & Diagnostic Tests				
Long-Run Rate Hike (β^{+}_{Low})	2.1450^{***} (0.4210)	—	—	—
Long-Run FX Depreciation (β^{+}_{FX})	9.4500^{***} (2.8500)	—	—	—
Long-Run Asymmetry Wald	$W = 14.82^{***}$ ($p = 0.0001$)	—	—	—
Pesaran Bounds F-statistic	$F = 7.82^{***}$ ($p < 0.01$)	—	—	—
First-Stage F-statistic	—	26.1^{***}	24.8^{***}	23.5^{***}
Hansen J Overid. p-value	—	0.485	0.531	0.498
R^2	0.7840	0.9554	0.9560	0.9548

$^{***},^{**},^{*}$ denote statistical significance at $1\%, 5\%, 10\%$. Standard errors in parentheses. Negative error-correction ($\lambda_{\text{ECT}} = -0.3210, t = -5.42, p < 0.0001$) confirms convergence at 32.1% per month. Bounds $F = 7.82$ exceeds the Pesaran et al. [29] $I(1)$ upper critical bound (4.66 at 1%).

The estimated error-correction coefficient ($\lambda_{\text{ECT}} = -0.3210, p < 0.0001$) implies a rapid disinflationary adjustment speed of 32.1% per month, translating to an empirical

half-life of disequilibrium absorption of:

$$\text{Half-Life} = \frac{\ln(0.5)}{\ln(1 - 0.3210)} \approx \mathbf{1.79} \text{ months} \quad (\approx 7.8 \text{ weeks}), \tag{C.1}$$

confirming that transitory monetary and cost-push deviations revert to their long-run asymmetric steady state in under two months.

Appendix D. Threshold Sensitivity Matrix and 24-Month Scenario Projections

Table D.9: Threshold Sensitivity and Functional Form Robustness Matrix

Specification / Model	**Threshold (i^*)**	**Cost Slope (ϕ^+_{Low})**	**Demand Slope (ϕ^+_{High})**	**Econometric Finding & Wald Test**
(1) Baseline Hansen (i_{t-1})	20.0%	1.8783^{***}	0.1232	Baseline threshold confirmed ($W = 19.84^{***}$)
(2) Polynomial Quadratic Model	20.01%	$\beta_1 = 3.642^{***}$	$\beta_2 = -0.091^{***}$	Implied Vertex $i^* = -\beta_1/(2\beta_2) = 20.01\%$
(3) Linear Splines Model	20.0%	1.8450^{***}	0.1180	Piecewise linear inversion at 20% ($p < 0.001$)
(4) Subsample Pre-2022 (2011–2021)	19.50%	1.7650^{***}	0.1410	Threshold invariant to 2022–2024 floatation
(5) Leave-COVID-Out (Excl. 2020)	20.0%	1.8910^{***}	0.1205	Invariant to pandemic supply disruptions
(6) Core CPI Inflation (CORE_t)	20.0%	1.6240^{***}	0.1080	Robust across non-food core basket

*** denotes statistical significance at 1%. All specifications control for exchange rate depreciation and foreign reserve buffers.

Table D.10: Multi-Scenario 24-Month Ahead Conditional Macroeconomic Projections

Horizon Month	**Baseline INFL**	**Sticky Reform**	**Stress Shock**	**Baseline EXCH**	**Stress EXCH**
$h = 1$ (May 2026)	10.80%	11.20%	11.80%	48.30	48.90
$h = 3$ (Jul 2026)	10.40%	11.00%	12.20%	48.70	49.50
$h = 6$ (Oct 2026)	9.80%	10.50%	12.50%	49.20	50.80
$h = 9$ (Jan 2027)	9.10%	10.00%	12.20%	49.80	52.00
$h = 12$ (Apr 2027)	8.50%	9.60%	11.80%	50.50	53.20
$h = 15$ (Jul 2027)	8.00%	9.30%	11.50%	51.10	54.10
$h = 18$ (Oct 2027)	7.50%	9.00%	11.20%	51.80	54.80
$h = 21$ (Jan 2028)	7.10%	8.80%	10.80%	52.30	55.40
$h = 24$ (Apr 2028)	6.80%	8.60%	10.50%	52.80	56.00

*** denotes statistical significance at 1%. *Scenario Notes:* All projections represent conditional illustrative scenario paths rather than deterministic point forecasts: (1) Baseline Path: PPP-aligned flexible exchange rate crawling float with gradual disinflation into the CBE target band ($7\% \pm 2\%$) and quarterly easing of 150–200 bps; (2) Sticky Reform Path: Accounts for administrative fuel/energy price adjustments causing inflation plateaus (8.6%–11.2%); (3) Stress Shock Path: Simulates external debt and regional liquidity pressures pushing exchange rates to 56.0 EGP/USD and reactivating pass-through ($\lambda^{+} = 8.2912$).